IEEJ Journal of Industry Applications
Vol.7 No.3 pp.250–258 DOI: 10.1541/ieejjia.7.250

Paper

Reaction Force Estimation of Electro-hydrostatic Actuator Using Reaction Force Observer

Kodai Umeda* Non-member, Tomoki Sakuma* Non-member
Kenta Tsuda* Non-member, Sho Sakaino* Senior Member
Toshiaki Tsuji* Senior Member

(Manuscript received July 13, 2017, revised Dec. 22, 2017)

Electro-hydrostatic actuators (EHAs) are hydraulic actuators that are flexible and exhibit high backdrivability. Flexible operation and accurate detection of reaction forces are required for robots to be able to perform in environments in which they will be cohabiting with humans. However, nonlinear elements that degrade detection accuracy, such as static friction, backlash, and oil leakage, are present in hydraulic systems. In addition, pressure sensors in hydraulic systems are not very accurate at estimating reaction forces, because they cannot estimate internal forces and viscous friction. In this study, we propose a combination of control algorithms for accurately estimating reaction forces. Static friction is compensated by using feedback modulators. In addition, we use a backlash and oil leakage compensator, which do not require any models, to suppress the relative velocity between the motor-side and load-side. Then, the use of a reaction force observer (RFOB) that exploits both pressure sensors and encoders is proposed. The RFOB can be implemented because disturbances are linearized by the compensators. Experimental results show that reaction forces can be estimated with very high accuracy using the proposed RFOB. In addition, we implemented force control using the RFOB and evaluate the force tracking performances by improving the estimation accuracy.

Keywords: electro-hydrostatic actuator, reaction force observer, feedback modulator, backlash compensation, oil leakage compensation

1. Introduction

The number of robots that cooperatively work alongside humans has been increased not only in industrial fields, but also in the nursing and rehabilitation fields. Because humans and robots are increasingly working on tasks together, they are expected to come into contact with each other. To make these interactions safe, robots need to be able to accurately detect external forces and flexibly move in response to unexpected disturbances. Thus, backdrivability, which is defined as the ability to respond to have low impedance characteristics with reaction forces, is required for robots to exhibit flexible motion.

Recently, robots have been able to perform increasingly diverse tasks because of advancements in automation. Hydraulic actuators have several advantages that make them suitable for use in robots, including a wide output power range and a compact drive system. Moreover, hydraulic actuators have a good power/weight ratio because their drive sources do not need to be located on robotic joints. Therefore, actuators allow more freedom in designing the configuration of the robot than electric actuators and many studies on the use of hydraulic actuators in robots have been reported [(1)–(3)]. Hydraulic actuators are driven by controlling the flow rate using servo-valves, and such drive circuits are popular in construction machinery [(4)]. However, these drive circuits are non-backdrivable because external forces are blocked by the servo-valves. In contrast, hydrostatic transmissions (HSTs) are hydraulic closed-circuits without servo-valves that allow backdrivability [(5)(6)]. To take advantage of the properties of both of these devices, electro-hydrostatic actuators (EHAs), which are HSTs driven by servo-pumps composed of electric servo-actuators and hydraulic pumps, have been developed. Bobrow *et al.* used an EHA to develop a multi-axis robot [(7)]. In recent years, robots utilizing the superior backdrivability of EHAs have been actively researched [(8)–(10)].

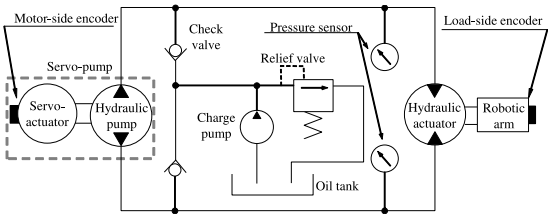

Fig. 1. The hydraulic circuit of an EHA

The hydraulic circuit of an EHA is shown in Fig. 1. Here, the motor-side contains an electric servo-actuator and a hydraulic pump, and the load-side is comprised of a hydraulic actuator and a robotic arm. In the motor-side, the output of the servo-actuator is directly coupled to the input of the hydraulic pump. The servo-actuator and hydraulic pump can rotate in both the forward and reverse directions. Consequently, oil flow from the pump to the hydraulic actuator is controlled by the servo-actuator, and rotation of the hydraulic actuator

* Graduate School of Science and Engineering, Saitama University
255, Shimo-ohkubo, Sakura-ku, Saitama 338-8570, Japan

can also be controlled. Using this mechanism, the hydraulic circuit forms a closed-loop because of the flow of oil. Therefore, EHAs are expected to have good backdrivability.

However, there are some nonlinear elements such as frictions, backlash, and oil leakage in hydraulic systems [11], and these elements degrade backdrivability. In other words, EHAs have acquired mechanical backdrivability, but there is still room for improvement in controlling the backdrivability. Besides, since these nonlinearities are caused by a plurality of factors, it is quite difficult to model accurately. Thus, it is necessary to control force based on reaction forces and compensate for such nonlinear elements without their accurate models in order to improve the control performance.

In hydraulic actuators, the force responses can be measured using pressure sensors instead of force sensors. Force sensing without force sensors is advantageous for preserving the rigidity of the actuators. However, pressure sensors cannot estimate internal forces and viscous friction. Consequently, the reaction force estimated by pressure sensors is not accurate, and this leads to decreases in force tracking performance. Thus, reaction force observers (RFOBs), which can estimate reaction force with high accuracy, are desired for EHAs. RFOBs are also useful tools estimating reaction forces without force sensors [12][13]. Generally, RFOBs are used with electric actuators because they have fewer nonlinear elements. Consequently, in order to implement RFOBs for EHAs, it is indispensable to compensate for nonlinear elements.

Previously, many studies have investigated methods to compensate for friction forces [14][15]. The friction forces in hydraulic circuits, especially the maximum static friction force, are dominant compared to the other actuators, such as electric and pneumatic actuators. Because of these characteristics, dead zones of no motion can occur at low speeds. Methods to compensate for friction, including the application of dithered signals and pulse-width modulation control, have been widely studied [16]. However, these methods are not suitable for EHAs because they rely on the response performance of servo-valves [17]. In order to overcome the problem of the dead zone, Sakaino *et al.* implemented feedback modulators (FMs) to control the hydraulic actuators [18][19]. Consequently, FMs are considered to be suitable for the practical implementation of EHAs. In this study, the dead zone caused by static friction was compensated using FMs as quantizers.

Backlash can lead to a loss of transmission [20][21]. Although compensation of backlash using a gear torque compensator has been studied [22], this method is difficult to use in hydraulic systems. This is because, not only margining between gears, but also the oil leakage, contribute to idling motion in hydraulic systems. In this paper, a backlash and oil leakage compensator (BLC) is proposed to suppress relative velocity between the motor-side and load-side of an EHA. The advantage of the proposed method is that idling motion caused by backlash and oil leakage can be compensated without separation. In addition, backlash and oil leakage inverse models, which have strong nonlinearity, are not required making the compensation easy to apply.

In this paper, an RFOB for EHAs is implemented because the disturbance characteristics were linearized due to the static friction, backlash, and oil leakage compensators. Then, we evaluated the accuracy of reaction force estimation in experiments using a developed EHA. In addition, force control using a FM, BLC, and RFOB was implemented to verify the improvement of the backdrivability of EHAs.

This paper is organized as follows. An experimental setup and a model of EHAs are shown in Section 2. In Section 3, the proposed method, which is an RFOB with static friction, backlash, and oil leakage compensators are described. The proposed method is experimentally verified in Section 4. Finally, this paper is concluded in Section 5.

2. Electro-hydrostatic Actuator

2.1 Experimental Setup Figure 2 shows the experimental setup used in this study, which consisted of a hydraulic actuator with a robotic arm that had one degree of freedom. A servo-pump and a charge unit are shown on the left side of Fig. 2. The servo-pump was coupled to the output shaft of the servo-actuator and the input shaft of the hydraulic pump. The rotation angle of the servo-actuator was measured by an absolute encoder with 17-bit resolution. A direct drive DC brushless motor (EC-60, made by MAXON) was used as a servo-actuator. A trochoid pump (MA-03, made by EATON) was used as a hydraulic pump. To supply oil to the hydraulic actuators, the charge unit was comprised of an oil tank, a relief valve, and a charge pump as a hydraulic source.

The right side of Fig. 2 shows the robotic arm that used an orbit motor (S-380, made by EATON) that we used as a hydraulic actuator. Here, a torque sensor (UTM-II, made by UNIPULSE) was inserted between the output shaft of the hydraulic actuator and the robotic arm. Note that the values measured using the torque sensor were only used for verification and were not used to provide any control and estimation in this study. The rotation angle of the hydraulic actuator was detected by an absolute encoder with 17-bit resolution.

2.2 Modeling Figure 3 shows the block diagrams representing the EHA. Figure 3(a) represents a model that has servo-actuators placed between the reference input electric current I^{ref} and the output angular response of the hydraulic pumps θ_m. Here, K_t is the torque constant, and τ_m^{dis} is the disturbance torque of the motor-side. J_m represents the moment of inertia of the servo-actuators on the motor-side. The models of servo-pump includes the model of static friction, in which intercepts the transmission of the input torque generated by the servo-actuators.

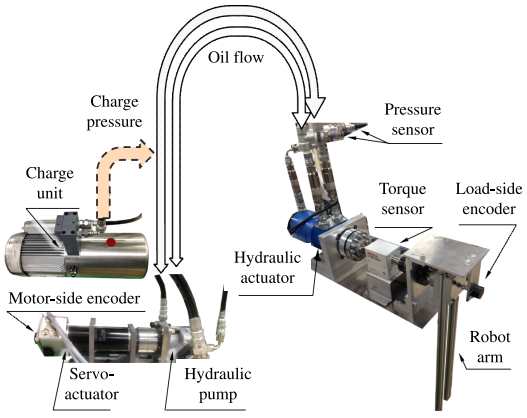

Fig. 2. Experimental setup

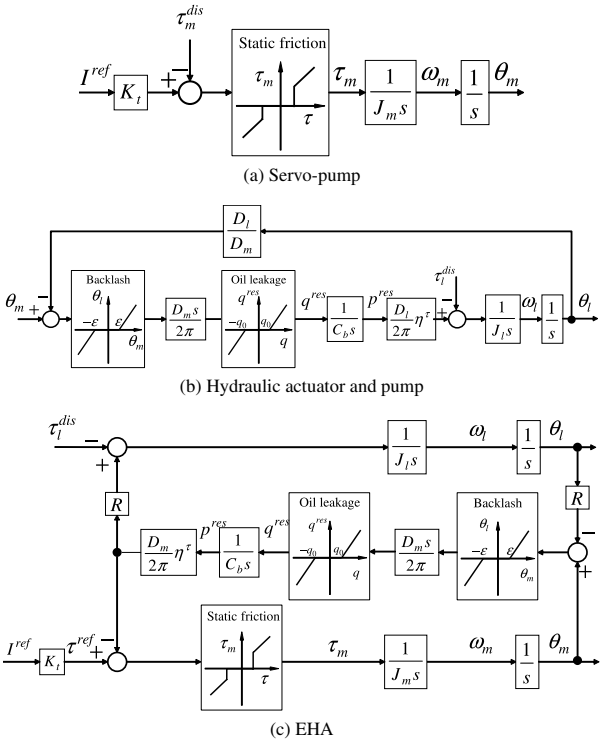

(a) Servo-pump

(b) Hydraulic actuator and pump

(c) EHA

Fig. 3. The block diagram of an EHA

Figure 3(b) is a block diagram of a model whose input is the rotation of the hydraulic pumps and whose output is the rotation of the hydraulic actuators. This model was described by Lee *et al.* [6].

Here, D_m and D_l refer to the displacement volumes of the hydraulic pumps and actuators, respectively. In addition, the volume displacement ratio of hydraulic pumps to actuators corresponds to the reduction ratio R as shown in (1).

$$R = \frac{D_l}{D_m} \cdots\cdots (1)$$

Note that nonlinear models of backlash and oil leakage were considered in the development of this model. As expressed (2), backlash width $\pm\epsilon$ can be calculated by integrating the relative angular velocity $\Delta\omega$.

$$\begin{aligned}\epsilon &= \left| \int (\omega_m - R\omega_l) \right| \\ &= \left| \int \Delta\omega \right| \cdots\cdots (2)\end{aligned}$$

Here, ω_m and ω_l are the angular velocity of the hydraulic pumps and hydraulic actuators, respectively. The oil leakage model q^{leak} is given as follows:

$$\begin{aligned}q^{leak} &= q - q^{res} = \frac{D_m}{2\pi}\omega_m - \frac{D_l}{2\pi}\omega_l \\ &= \frac{D_m}{2\pi}\Delta\omega \cdots\cdots (3)\end{aligned}$$

where q is the supply oil flow from the hydraulic pumps and q^{res} is the input oil flow to the hydraulic actuators. Then, p^{res} is the pressure difference between the input and output ports of the hydraulic actuator. τ_l^{dis} is the disturbance torque of the load-side, and η^τ is the torque efficiency. C_b refers to the compression coefficient of oil, and J_l represents the moment of inertia of the hydraulic actuators.

When the servo-actuators and hydraulic pumps are combined, the disturbance torque of the motor-side is given by (4).

$$\tau_m^{dis} = \frac{D_m}{2\pi}\eta^\tau p^{res} \cdots\cdots (4)$$

Consequently, a model of an entire EHA can be designed as shown in Fig. 3(c) by combining Fig. 3(a) and (b). As described above, the EHA includes a plurality of nonlinear models: static friction, backlash, and oil leakage. These nonlinear models are not correct, and in reality they have more complicated nonlinearities. However, strict modeling of the nonlinear elements is not needed in this study.

3. Controllers for Reaction Force Observer

Assuming that inertia and friction in EHAs are sufficiently small, reaction torques are estimated as shown in (5).

$$\hat{\tau}^{reac} = \frac{D_l}{2\pi}p^{res} - J_l\dot{\omega}_l - \tau^f \simeq \frac{D_l}{2\pi}p^{res} \cdots\cdots (5)$$

Here, τ^f is friction torque. From (5), reaction torques can be estimated by pressure value. Conventionally, reaction force estimation based on (5) has been used [23][24]. However, there are disturbance torques, which cannot be detected by pressure value. For example, there is a dead zone due to torque from static friction that is caused by internal oil leakage in the low speed range, and these characteristics are known to have nonlinearities. Therefore, the reduction in output efficiency is nonlinear, and it is impossible to estimate the exact reaction torque. Furthermore, hydraulic motors, especially gear motors, exhibit backlash between the gears of the load and drive shafts. There is a non-contact state that allows backlash to occur, when the motors switch their rotation.

RFOBs can estimate reaction forces by considering disturbance torques such as internal force and friction using pressure sensors and encoders. Conventionally, RFOBs have been designed for electric motors, and the inputs of RFOBs are reference currents that go into the motor-side [25]. However, RFOBs cannot be implemented into EHAs without compensating for nonlinear elements such as static friction, backlash, and oil leakage. Therefore, nonlinearity compensators, specifically the FM and BLC, are proposed to allow RFOBs to be implemented.

3.1 Feedback Modulator

Static friction in EHAs is very large compared to other actuators, and dead zones occur in the low-speed range. In order to drive hydraulic pumps that are affected by static friction, the input torque must be greater than the maximum static friction force. Dither signals are commonly used to compensate for static friction. However, models of static friction are needed to improve performance. Recently, Ohghi *et al.* proved that feedback modulators (FMs) can effectively suppress the effects of static friction [17]. Input torques are quantized so that they exceed the maximum static friction force while the effect of the quantization error is suppressed by the use of FMs. FMs are dynamic quantizers and exhibit high robustness because models of systems are unnecessary.

A block diagram of FMs is shown in Fig. 4. Here, the filter $Q(s)$ confirms $1 - Q(s) = (Ts/Ts+1)^2$, and the time constant

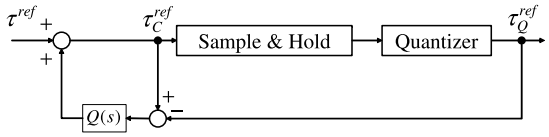

Fig. 4. Block diagram of a feedback modulator

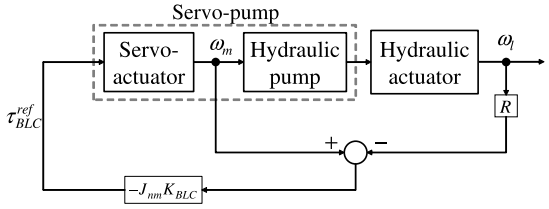

Fig. 5. The block diagram of an BLC

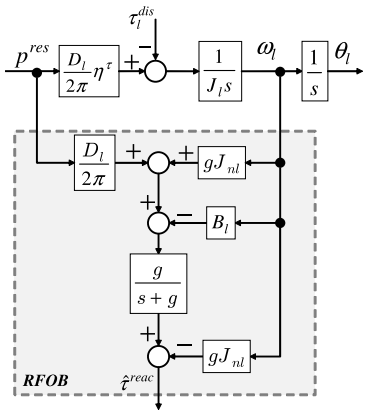

Fig. 6. The block diagram of an RFOB for EHA

T is represented by $T = aST$, where a is a positive constant, and ST is the sampling time, respectively. In addition, the reference input torque τ^{ref} and its quantized value τ_Q^{ref} confirm the following equation:

$$\tau_Q^{ref} = \begin{cases} \tau^{ref} + (1 - Q(s))\, e & (|\omega_l| < \omega_{th}) \\ \tau^{ref} & (|\omega_l| \geq \omega_{th}) \end{cases} \cdots\cdots\cdots (6)$$

where $e = \tau_C^{ref} - \tau_Q^{ref}$ and ω_{th} is the threshold of angular velocity. It should be noted that using this method, the reference torque is only quantized when the motor's speed is low. Note that FMs do not affect the stability of the entire control system so that interference between FMs and the other controllers does not need to be considered [19].

3.2 Backlash and Oil Leakage Compensator There is backlash which causes nonlinearities in EHAs using gear motors, and backlash causes idling motion. This backlash results from margining between gears. In addition, assembly errors and oil leakage also cause effects similar to those of backlash. Therefore, idling motion is particularly increased in hydraulic actuators. Because torque is not transmitted from the load-side to the motor-side during idling motion, compensation is necessary.

However, it is quite difficult to create a model-based compensator such as the joint torque control proposed by Yamada *et al.* [26] because of the complexity of modeling hydraulic systems. From (2) and (3), backlash and oil leakage can be observed as relative velocity between the load-side and the motor-side $\Delta\omega$. Hence, if the relative velocity is controlled to be zero, the effect of idling motion on the force controller are minimal. Therefore, a BLC is proposed as shown in Fig. 5.

Then, the control input of the BLC is shown in (7).

$$\tau_{BLC}^{ref} = -K_{BLC} J_{nm} \Delta\omega \cdots\cdots\cdots (7)$$

In (7), K_{BLC} is the feedback gain, and J_{nm} is the moment of inertia of the servo-pumps. Note that relative position cannot be accounted for in this compensation because the offsets of the initial points in the backlash must be known. Of course, these are difficult to identify.

Here, we describe the effect in EHAs with the use of the proposed compensator. When static friction can be neglected by the use of FMs, the equation of motion is expressed as follows:

$$J_m \dot{\omega}_m = -K_{BLC} J_{nm} \Delta\omega - \frac{D_m}{2\pi} \eta^\tau p^{res} \cdots\cdots\cdots (8)$$

$$J_l \dot{\omega}_l = \frac{D_l}{2\pi} \eta^\tau p^{res} - \tau_l^{dis}. \cdots\cdots\cdots (9)$$

From (8) and (9), assuming that there are no modeling errors ($J_{nm} = J_m$), the differential equation of the BLC is expressed by the following equation.

$$\begin{aligned} \Delta\dot{\omega} &= \dot{\omega}_m - R\dot{\omega}_l \\ &= -K_{BLC}\Delta\omega + C \cdots\cdots\cdots (10) \end{aligned}$$

Here, $C = \frac{R\tau_l^{dis}}{J_l} - \frac{D_m}{2\pi}\left(\frac{1}{J_m} + \frac{R^2}{J_l}\right)\eta^\tau p^{res}$. Considering the disturbance term as a step function, C is a constant value. From (10), the proposed controller can compensate backlash and oil leakage in the velocity dimension by linear differential equation of the relative velocity. In addition, since the BLC is expressed by the first order linear differential equation, it is possible to compensate backlash and oil leakage without affecting the stability of EHAs.

3.3 Reaction Force Observer RFOBs are based on disturbance observers [13]. In hydraulic actuators, the pressure difference between the input and output ports of the hydraulic actuator p can be treated as an input. Because static friction, backlash, and oil leakage were compensated by the BLC and FM, the estimated disturbance torque of the load-side can be modeled using the following equation.

$$\hat{\tau}_l^{dis} = \hat{\tau}^{reac} + \hat{\tau}^f + \frac{D_l}{2\pi}\Delta\eta^\tau p^{res} \cdots\cdots\cdots (11)$$

From (11), the estimated disturbance torque includes reaction torque $\hat{\tau}^{reac}$, viscous friction torque $\hat{\tau}^f$, and variation of torque efficiency $\Delta\eta^\tau p^{res}$. Torque efficiency is a nonlinear function with respect to velocity and it is difficult to estimate its variation in real time. Therefore, assuming that $\eta^\tau = 1$ and there are no variations, (11) can be approximated as (12).

$$\hat{\tau}_l^{dis} \simeq \hat{\tau}^{reac} + \hat{\tau}^f \cdots\cdots\cdots (12)$$

Here, $\hat{\tau}^f$ is the viscous friction which is defined as follows.

$$\hat{\tau}^f = B_l \omega_l \cdots\cdots\cdots (13)$$

B_l is the viscous coefficient of the load-side, which should be identified. By combining (12) and (13), the estimated reaction torque is calculated as follows:

$$\hat{\tau}^{reac} = \frac{g}{s+g}\left(\frac{D_l}{2\pi} p^{res} - J_{nl}\dot{\omega}_l - \hat{\tau}^f\right) \cdots\cdots\cdots (14)$$

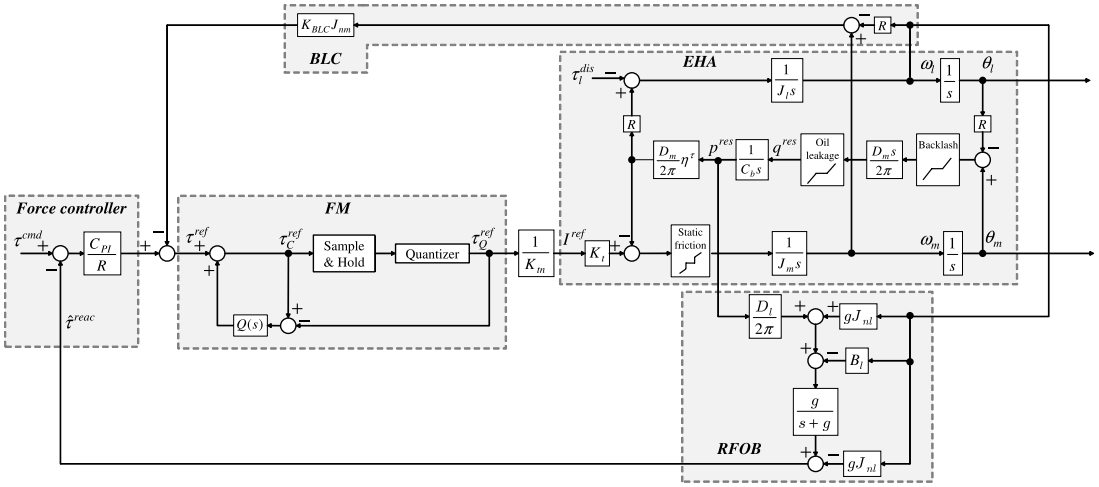

Fig. 7. The entire block diagram of the control loop

where g is the cutoff frequency of the RFOB, and J_{nl} is the nominal moment of inertia of the hydraulic actuators. As described above, the proposed RFOB requires a pressure difference, angular acceleration, and angular velocity to estimate the torque reaction, and only pressure sensors and encoders are required for these measurements. A block diagram of the proposed RFOB is shown in Fig. 6.

4. Experimental Validation

This section presents the experimental results that were used to verify the compensators and observers. First, the performance of the compensators described in Section 3.2 and 3.1 is discussed in Section 4.1. Then, the RFOB shown in Section 3.3 was implemented in the EHA, and the estimation accuracy was evaluated in Section 4.2.

Furthermore, backdrivability was verified using force control with the proposed method in Section 4.3. In the experiment, a proportional-integral (PI) controller was implemented, as this is what is used in hydraulic force control [27]. The force controller was based on conventional force control methods [4]. Of course, sliding mode control [28], backstepping control [29], and any other control methods [30]–[32] can be applied as force controllers using the proposed RFOB. However, because designing of force controllers is not contribution of this study, the PI controller was used for its simpleness.

The experimental setup was described in Section 2.1. The angular velocities of the motor-side and load-side were calculated by pseudo-derivation. Pressure and torque values were passed through a low-pass filter to remove of sensor noise. The parameters are shown in Table 1, and Fig. 7 shows the entire block diagram of the proposed experimental controller. In this figure, the backlash and oil leakage compensator is labeled as *BLC*, the feedback modulator is *FM* and the reaction force observer is *RFOB*. In the force controller, C_{PI} is represented by $C_{PI} = K_p + K_i \frac{1}{s}$.

4.1 Backlash and Oil Leakage Compensator and Feedback Modulator In this experiment, we verified the relationship between the angular velocity of the motor-side and the reaction torque during backdriving motion. When external torque was applied to the robot arm, rotation of the motor-side was measured as the output. Reaction torque was measured using the torque sensor as the input, and angular velocity was calculated from the angular response that was measured using the motor-side encoder. Time series results of the compensation for the nonlinear elements are shown in Fig. 8. In this figure, the vertical axis shows the reaction torque, and the horizontal axis shows the angular velocity of the motor-side encoder. Therefore, this figures shows the rotation of the motor-side that was obtained by backdriving.

Table 1. Parameters

J_{nm}	Nominal inertia of motor-side [kgm^2]	0.00044
J_{nl}	Nominal inertia of load-side [kgm^2]	0.0140
B_l	Viscous coefficient of load-side [Nms/rad]	4.56
D_m	Displacement volume of hydraulic pump [cm^3/rev]	3.08
D_l	Displacement volume of hydraulic actuator [cm^3/rev]	371
R	Reduction ratio	120
K_{tn}	Torque constant of servo-actuator [Nm/A]	0.147
K_a	BLC gain	120
K_p	Proportional gain of the force controller	1.50
K_i	Integral gain of the force controller	0.500
τ_{cmd}	Command torque [Nm]	0
ω_{th}	Threshold of angular velocity [rad/s]	0.200
g_p	Cut-off frequency of pressure sensor [rad/s]	20.0
g_{tr}	Cut-off frequency of torque sensor [rad/s]	20.0
g_{pd}	Cut-off frequency of pseudo-derivation [rad/s]	40.0
g_{rfob}	Cut-off frequency of RFOB [rad/s]	20.0
ST	Sampling time [ms]	1.00

Figure 8(a) shows that 33 Nm of torque was needed to backdrive without any compensation. This was the maximum static friction torque of the EHA. Figure 8(b) shows that the torque required for backdriving was reduced to 1.3 Nm when the BLCs were added. However, the compensator overcompensated when the input torque exceeded the static friction torque. Therefore, static friction cannot be dealt with by the BLC alone. Figure 8(c) shows the results when both the BLC and FM were utilized. Since static friction torque was compensated by the FM, there was an approximately linear relationship, similar to what would be produced by viscous friction, between the measured motor-side angular velocity and the input torque. Slightly nonlinearity for velocity-torque characteristic is observed around 0.05 rad/s. This is because BLC can reduce idling motion caused by backlash and oil leakage, but it is impossible to completely remove mechanical nonlinearity. In addition, this slightly nonlinearity has little influence on reaction torque estimation. In summary, the

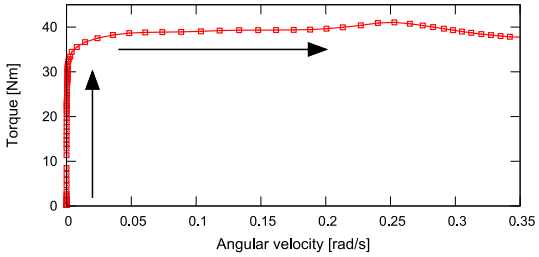

(a) Without compensators

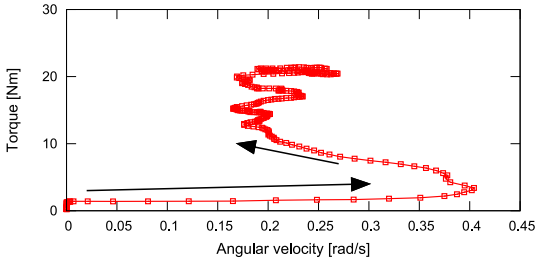

(b) BLC

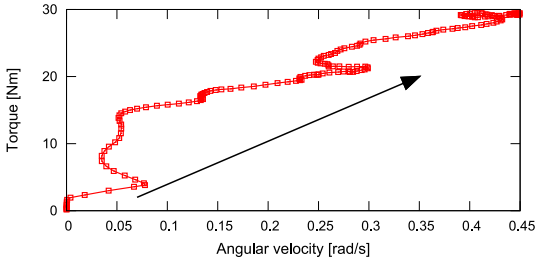

(c) BLC + FM

Fig. 8. Velocity-torque characteristics without force control during backdriving motion

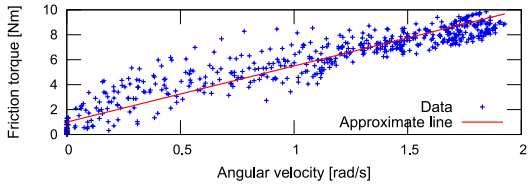

Fig. 9. Estimation of the coefficient of viscous friction

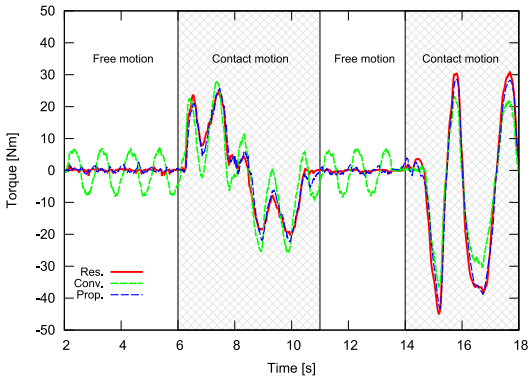

(a) Reaction torque

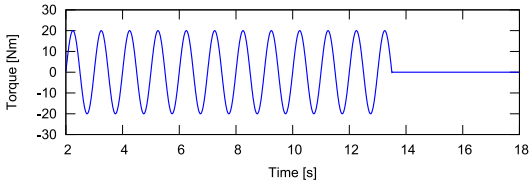

(b) Torque input of servo-actuator

Fig. 10. Experimental result of reaction torque estimation

BLC reduced the backdrive torque, and the FM linearized the responses. The complicated nonlinearities, specifically static friction, backlash, and oil leakage were successfully transformed into a disturbance that was easier to deal with, viscous friction torque.

4.2 The Proposed RFOB First, the viscous friction was identified. Sine-wave inputs with the use of the FM and BLC were applied as given in the following equation.

$$\tau^{ref} = 40\sin(2\pi f t) + \tau^{ref}_{BLC}$$

Here, $f = 1\,\mathrm{Hz}$ was the input frequency and t is time. The moment of inertia of motor-side and load-side are identified by following equations.

$$J_{nm} = \left(\frac{\tau^{ref}_Q}{R} - \frac{D_m}{2\pi}p^{res}\right)/\dot{\omega}_m \quad \cdots\cdots (15)$$

$$J_{nl} = \left(\frac{D_l}{2\pi}p^{res} - \hat{\tau}^{dis}_l\right)/\dot{\omega}_l \quad \cdots\cdots (16)$$

Viscous friction torque was obtained from the pressure values and angular velocity. B_l was represented identified as the following equation using Eqs. (12), (13), and (16) since $\hat{\tau}^{reac} = 0$ in free motion.

$$B_l\omega_l = \frac{D_l}{2\pi}p^{res} - J_{nl}\dot{\omega}_l \quad \cdots\cdots (17)$$

Figure 9 shows the relationship between angular velocity on the load-side and viscous friction torque. The measured values are shown with the points and the line denotes the linear approximation. The slope of the line was 4.56 Nms/rad, and this was the viscous friction coefficient B_l.

Next, we verified the accuracy of the reaction torque estimation. The RFOB was implemented in EHAs using the viscous friction model we identified. In this experiment, the force controller was turned off, and the BLC and FM were turned on. τ^{ref} is expressed by the following equation.

$$\tau^{ref} = \begin{cases} 20\sin(2\pi f t) + \tau^{ref}_{BLC} & (2.0 \le t < 13.5) \\ \tau^{ref}_{BLC} & (13.5 \le t) \end{cases} \quad \cdots\cdots (18)$$

A comparison between the methods of the reaction torque estimation is shown in Fig. 10(a). Here, three lines show the reaction torque responses: the red line shows the value measured by the torque sensor (Res.), the green line shows the estimated value using the pressure sensors (Conv.), and the blue line shows the estimated torque using the RFOB (Prop.). Figure 10(b) shows torque input in Fig. 10(a). In Fig. 10(a), from 6 to 11 seconds, and from 14 to 18 seconds, external torque was applied by a subject pressing the robot arm as contact motion. While sine-waves were applied, the conventional method could not separate the input torque and reaction torque, and a large error from the response of reaction torque remained. These errors did not appear in the proposed method, and more accurate reaction torque was estimated. Root mean square errors (RMSEs) associated with each method are shown in Table 2. The RMSEs using the pressure sensors and the RFOB were 5.23 Nm and 1.89 Nm,

Table 2. Root mean square error of torque estimation

Estimated method	RMSE [Nm]
Pressure conversion (Conv.)	5.23
The proposed RFOB (Prop.)	1.89

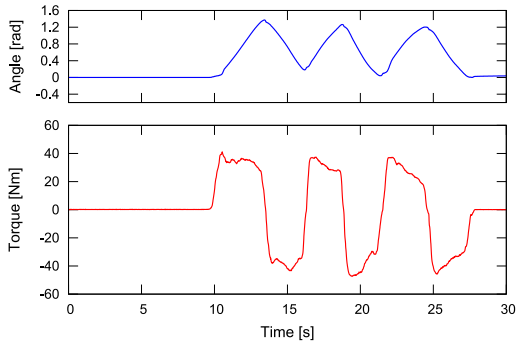

(a) Without force control

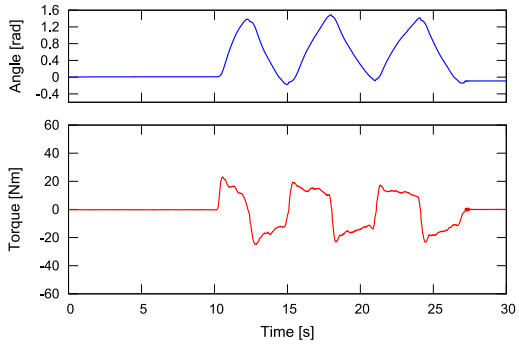

(b) Force control using pressure (Conv.)

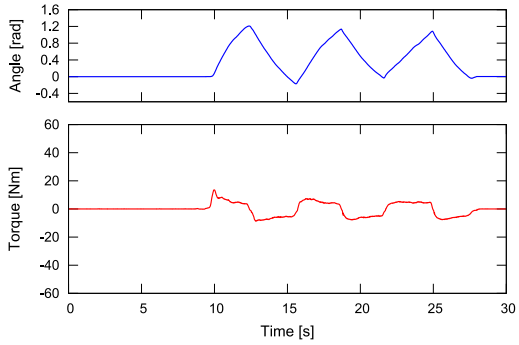

(c) Force control using the RFOB with BLC + FM (Prop.)

Fig. 11. Reaction torque and angular response during backdriving motion

respectively. These results clearly verified that the proposed RFOB had superior reaction torque estimation performance.

In general, RFOBs are affected by backlash around 0 Nm. However, in Fig. 10(a), it was shown that the reaction force was estimated accurately even in such states, due to compensation for the nonlinearities. On the other hand, using the proposed methods, pulsating errors occurred around the maximum input torque. These errors resulted from a reduction in the torque efficiency η^{τ}. More research is needed in order to determine how to obtain more accurate characteristics.

4.3 Force Control with the RFOB Through these experiments, the effect of force control was verified, and the ability of force control to improve backdrivability was evaluated. Figure 11 shows the reaction torque response that was measured by the torque sensor during backdriving motion. During backdriving motion, we gave an external torque to the robot causing forward and reverse rotation, and the angular responses are also shown at the top of each figure. Figure 11(a) shows the results we obtained when the robot was backdriven without the use of force control. Figure 11(b) and (c) show the results obtained when the robot was backdriven with the use of force control by using pressure (Conv.) and the proposed RFOB (Prop.), respectively. In addition, RMSEs between the command torque and reaction torque when each method was employed are shown in Table 3.

Table 3. Root mean square error of force control

		RMSE [Nm]
Without force control		24.3
With force control	using pressure (Conv.)	10.7
	using the RFOB (Prop.)	4.18

Comparing Fig. 11(a) and (b), it is clear that the operator needed a smaller torque to manipulate the robots when force control was implemented. Here, the RMSEs associated with the data shown in Fig. 11(a) and (b) were 24.3 Nm and 10.7 Nm, respectively. In addition, Fig. 11(c) shows that the operation torque was reduced to 4.18 Nm when the proposed method was used because the torque was accurately estimated. These results clearly verified that the backdrivability of robots was improved when the proposed RFOB was used to provide force control. Note that there was residual torque in free motion that was caused by inertial torque and viscous friction torque. A previous study indicates that the effect of viscous friction can be compensated by a feedforward compensator [14]. To achieve even better performance, we will try to implement this compensator in the future.

5. Conclusion

Backlash, oil leakage, and static friction in EHAs decrease the backdrivability of these devices. To solve this problem, we proposed a combination of three controllers as a highly accurate reaction force estimation method in EHAs on the premise of using force control: reaction force observer, backlash and oil leakage compensation, static friction compensation. To realize the RFOB implementation, the BLC and FM were utilized to overcome backlash and oil leakage, and static friction, respectively. The effects of the nonlinear elements, backlash, oil leakage, and static friction, were linearized and so they behaved like viscous friction. Consequently, we confirmed that highly accurate reaction force estimation of EHAs using the RFOB is possible. In addition, the proposed RFOB can be implemented in other hydraulic actuators. Finally, a force controller comprised of the RFOB, BLC, and FM was applied to the EHA. Experimental results demonstrated that there was a drastic improvement in backdrivability when the proposed method was implemented. We believe that this method is the key to safe and flexible robot operation.

Acknowledgment

This research was supported by JSPS KAKENHI Grant Number 16K06410.

References

(1) M. Raibert, K. Blankespoor, G. Nelson, and R. Playter: "Bigdog, the rough-terrain quadruped robot", *IFAC Proceedings Volumes*, Vol.41, No.2, pp.10822–10825 (2008)

(2) J.P. Whitney, T. Chen, J. Mars, and J.K. Hodgins: "A hybrid hydrostatic transmission and human-safe haptic telepresence robot", Disney Research (2016)

(3) M. Focchi, G.A. Medrano-Cerda, T. Boaventura, M. Frigerio, C. Semini, J. Buchli, and D.G. Caldwell: "Robot impedance control and passivity analysis with inner torque and velocity feedback loops", *Control Theory and Technology*, pp.1–16 (2016)

(4) A.G.L. Junior, R.M. de Andrade, and A. Bento Filho: "Linear serial elastic hydraulic actuator: Digital prototyping and force control", *IFAC-PapersOnLine*, Vol.48, No.6, pp.279–285 (2015)

(5) H. Kaminaga, T. Yamamoto, J. Ono, and Y. Nakamura: "Backdrivable miniature hydrostatic transmission for actuation of anthropomorphic robot hands", in 2007 7th IEEE-RAS International Conference on Humanoid Robots, pp.36–41, IEEE (2007)

(6) W.Y. Lee, M.J. Kim, and W.K. Chung: "An approach to development of electro hydrostatic actuator (eha)-based robot joints", in Industrial Technology (ICIT), 2015 IEEE International Conference on, pp.99–106 (2015)

(7) J.E. Bobrow and J. Desai: "Modeling and analysis of a high-torque, hydrostatic actuator for robotic applications", in Experimental Robotics I, pp.215–228 (1990)

(8) H. Kaminaga, T. Yamamoto, J. Ono, and Y. Nakamura: "Anthropomorphic robot hand with hydrostatic actuators", in Proc. of 7th IEEE-RAS Int'l Conf. on Humanoid Robots, pp.36–41 (2007)

(9) H. Kaminaga, J. Ono, Y. Nakashima, and Y. Nakamura: "Development of backdrivable hydraulic joint mechanism for knee joint of humanoid robots", in ICRA'09. IEEE International Conference on Robotics and Automation, 2009, pp.1577–1582 (2009)

(10) K. Tsuda, T. Sakuma, K. Umeda, S. Sakaino, and T. Tsuji: "Resonance-suppression control for electro-hydrostatic actuator as two-inertia system", *IEEJ Journal of Industry Applications*, Vol.6, No.5, pp.320–327 (2017)

(11) M. Yonemochi: "Characteristics of load transmission mechanisms of hydraulic control systems", *Transactions of the Society of Instrument and Control Engineers*, Vol.1, pp.274–281 (1965)

(12) T. Murakami, R. Nakamura, F. Yu, and K. Ohnishi: "Force sensorless compliant control based on reaction force estimation observer in multi-degrees-of-freedom robot", *Journal of RSJ*, Vol.11, No.5, pp.765–768 (1993)

(13) S. Katsura, Y. Matsumoto, and K. Ohnishi: "Modeling of force sensing and validation of disturbance observer for force control", *IEEE Transactions on Industrial Electronics*, Vol.54, No.1, pp.530–538 (2007)

(14) Y. Sang, H. Gao, and F. Xiang: "Practical friction models and friction compensation in high-precision electro-hydraulic servo force control systems", *Instrumentation Science & Technology*, Vol.42, No.2, pp.184–199 (2014)

(15) H. Kaminaga, K. Odanaka, Y. Ando, S. Otsuki, and Y. Nakamura: "Evaluations on contribution of backdrivability and force measurement performance on force sensitivity of actuators", in 2013 IEEE/RSJ International Conference on Intelligent Robots and Systems, pp.4472–4477 (2013)

(16) H. Kato, T. Nishiumi, and T. Ichiyanagi: "Improvement of angular position control characteristics for a hydraulic motor with dead zone by means of a nural network and surperimposed small oscillation", *Transactions of the Japan Fluid Power System Society*, Vol.35, No.5, pp.89–96 (2004)

(17) T. Ohgi and Y. Yokokohji: "Control of hydraulic actuator systems using feedback modulator", *Journal of Robotics and Mechatronics*, Vol.20, No.5, p.695 (2008)

(18) S. Sakaino and T. Tsuji: "Oil leakage and friction compensation for electro-hydrostatic actuator using drive-side and load-side encoders", in The 42th International Conference on Industrial Electronics, Control and Instrumentation (IECON' 16) (2016)

(19) S. Sakaino and T. Tsuji: "Development of friction free controller for electro-hydrostatic actuator using feedback modulator and disturbance observer", *ROBOMECH Journal*, Vol.4, No.1, p.1 (2017)

(20) J. Vörös: "Modeling and identification of systems with backlash", *Automatica*, Vol.46, No.2, pp.369–374 (2010)

(21) L. Márton and B. Lantos: "Control of mechanical systems with stribeck friction and backlash", *Systems & Control Letters*, Vol.58, No.2, pp.141–147 (2009)

(22) M. Odai and Y. Hori: "Speed control of 2-inertia system with gear backlash using gear torque compensator", in Advanced Motion Control, 1998. AMC'98-Coimbra., 1998 5th International Workshop on, pp.234–239 (1998)

(23) K. Tsuda, S. Sakaino, and T. Tsuji: "Bilateral control between electric and electro-hydrostatic actuators using feedback modulator", in Industrial Electronics Society, IECON 2016-42nd Annual Conference of the IEEE, pp.506–511, IEEE (2016)

(24) S. Sakaino, T. Furuya, and T. Tsuji: "Bilateral control between electric and hydraulic actuators using linearization of hydraulic actuator", *IEEE Transactions on Industrial Electronics*, Vol.64, No.6, pp.4631–4641 (2017)

(25) T. Murakami, F. Yu, and K. Ohnishi: "Torque sensorless control in multidegree-of-freedom manipulator", *IEEE Transactions on Industrial Electronics*, Vol.40, No.2, pp.259–265 (1993)

(26) S. Yamada, K. Inukai, H. Fujimoto, K. Omata, Y. Takeda, and S. Makinouchi: "Joint torque control for two-inertia system with encoders on drive and load sides", in 2015 IEEE 13th International Conference on Industrial Informatics (INDIN), pp.396–401 (2015)

(27) H. Kaminaga, T. Kang, and Y. Nakamura: "Force control of an electro-hydraulic actuator using moter velocity control", in Proceedings of the 2014 JSME Conference on Robotics and Mechatronics, pp.1A1–I04(1)–1A1–I04(4) (2014)

(28) W.M. Bessa, M.S. Dutra, and E. Kreuzer: "Sliding mode control with adaptive fuzzy dead-zone compensation of an electro-hydraulic servo-system", *Journal of Intelligent and Robotic Systems*, Vol.58, No.1, pp.3–16 (2010)

(29) H. Kim, S. Park, J. Song, and J. Kim: "Robust position control of electro-hydraulic actuator systems using the adaptive back-stepping control scheme", *Proceedings of the Institution of Mechanical Engineers, Part I: Journal of Systems and Control Engineering*, Vol.224, No.6, pp.737–746 (2010)

(30) A. Alleyne and R. Liu: "A simplified approach to force control for electro-hydraulic systems", *Control Engineering Practice*, Vol.8, No.12, pp.1347–1356 (2000)

(31) K.K. Ahn and Q.T. Dinh: "Self-tuning of quantitative feedback theory for force control of an electro-hydraulic test machine", *Control Engineering Practice*, Vol.17, No.11, pp.1291–1306 (2009)

(32) M. Namvar and F. Aghili: "A combined scheme for identification and robust torque control of hydraulic actuators", *Journal of dynamic systems, measurement and control*, Vol.125, No.4, pp.595–606 (2003)

Kodai Umeda (Non-member) received the B.E. degree in the electrical and electronic systems from Saitama University, Saitama, Japan, in 2016. He is currently working on M.E. degree at the Department of Electrical and Electronic Systems from Saitama University. His research interests include motion control and mechatronics.

Tomoki Sakuma (Non-member) received the B.E. and M.E. degrees in the electrical and electronic systems from Saitama University, Saitama, Japan, in 2015, and 2017, respectively. He currently works at KAWASAKI HEAVY INDUSTRIES.

Kenta Tsuda (Non-member) received the B.E. degree in the electrical and electronic systems from Saitama University, Saitama, Japan, in 2016. He is currently working on M.E. degree at the Department of Electrical and Electronic Systems from Saitama University. His research interests include motion control and mechatronics.

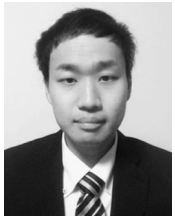

Sho Sakaino (Senior Member) received the B.E. degree in system design engineering and the M.E. and Ph.D. degrees in integrated design engineering from Keio University, Yokohama, Japan, in 2006, 2008, and 2011, respectively. He is currently an assistant professor with the Department of Electrical and Electronic Systems, Saitama University and JST, PRESTO. His research interests include mechatronics, motion control, robotics, and haptics. He received the IEEJ Industry Application Society Distinguished Transaction Paper Award in 2011.

Toshiaki Tsuji (Senior Member) received the B.E. degree in system design engineering and the M.E. and Ph.D. degrees in integrated design engineering from Keio University, Yokohama, Japan, in 2001, 2003, and 2006, respectively. He was a research associate in Department of Mechanical Engineering, Tokyo University of Science from 2006 to 2007. He is currently an associate professor with the Department of Electrical and Electronic Systems, Saitama University, Saitama, Japan. His research interests include mechatronics, motion control, haptics, and rehabilitation robots. He received the FANUCFA and Robot Foundation Original Paper Award in 2007 and 2008.